Contribution of local atomic arrangements and electronic structure to high electrical resistivity in the $Al_{82.6-x}Re_{17.4}Si_x$ ($7 \leqslant x \leqslant 12$) 1/1-1/1-1/1 approximant

T. Takeuchi

Research Center for Advanced Waste and Emission Management, Nagoya University, Nagoya 464-8603, Japan

T. Onogi, T. Otagiri, and U. Mizutani

Department of Crystalline Materials Science, Nagoya University, Nagoya 464-8603, Japan

H. Sato

Department of Physics, Aichi University of Education, Nagoya 464-8603, Japan

K. Kato

Japan Synchrotron Radiation Research Institute, Hyogo 679-5198, Japan

T. Kamiyama

Neutron Science Laboratory, Institute of Materials Structure Science, High Energy Accelerator Research Organization, Tsukuba 305-0801, Japan

Electrical resistivity of $Al_{82.6-x}Re_{17.4}Si_x$ ($7 \leqslant x \leqslant 12$) 1/1-1/1-1/1 approximants was discussed in terms of their electronic structure near the Fermi level and the local atomic arrangements. Strong composition dependence of the electrical resistivity was observed for these 1/1-1/1-1/1 approximants; samples with $x=7$, 9, and 12 show the Boltzmann-type electrical resistivity, while the others possess behaviors expected for system under the weak-localization. We found that the weak localization effect in the electrical resistivity, which is one of the characteristics of the corresponding Al-based quasicrystals, appears only when a condition of very low density of states with imperfections in the periodicity is satisfied. The Boltzmann-type behavior, on the other hand, takes place when one of the two factors, the very low density of states or the imperfection in the periodicity, is absent from the structure of the 1/1-1/1-1/1 approximant.

I. INTRODUCTION

After the discovery of thermodynamically stable quasicrystals,[1–3] physical properties associated with the quasiperiodicity have been investigated with use of these stable quasicrystals of very high structural quality. An insulating behavior in electrical resistivity observed for the Al-Pd-Re icosahedral quasicrystal[4] and very high-electrical resistivities for other icosahedral phases, such as Al-Cu-Fe, Al-Cu-Ru, Al-Pd-Mn, and Al-Pd-Os quasicrystals,[5] are the most pronounced characteristics that are widely believed to be introduced by the quasiperiodicity in the quasicrystalline structure. The role of quasiperiodicity in increasing electrical resistivity, however, has not been well understood yet, because no clear explanation has been proposed on an open question "why some crystalline approximants possess a very high electrical resistivity even without the quasiperiodicity in their structure?" The high electrical resistivity reaching nearly 10 000 $\mu\Omega$ cm observed for the Al-Re-Si 1/1-1/1-1/1 approximant[6] is one of the most typical examples. Relatively low electrical resistivities about 150–200 $\mu\Omega$ cm observed for Al-Mg-Zn, Mg-Zn-Y, and Cd-Yb icosahedral quasicrystals of high structure quality[7–10] also conflict with the scenario of the critical role of the quasiperiodicity in increasing their electrical resistivity.

In order to find the most important factors leading the high electrical resistivity characteristic to some icosahedral quasicrystals and their approximants, we decided not to employ quasicrystals but crystalline approximants because approximants possess the similar local atomic arrangements and electronic structure as those in the corresponding quasicrystals due to their relation in the high-dimensional space,[11] and because the electronic structure and the local atomic arrangements of the approximants can be precisely determined by the conventional band-calculation and structure analyses well developed for crystalline materials. The roles of local atomic arrangements and of the electronic structure in increasing their electrical resistivity can be investigated by making full use of the atomic and electronic structure analyses on the crystalline approximants. Moreover, we can also reveal the effects of the quasiperiodicity on the electrical conductivity by comparing the electrical properties of the quasicrystals with those of the corresponding approximant.

In this study, we employed a series of Al-Re-Si 1/1-1/1-1/1 approximants possessing very high electrical resistivities up to 10 000 $\mu\Omega$ cm at 2 K. The local atomic arrangements were determined by the synchrotron-radiation and neutron Rietveld analyses, and the density of states at the Fermi level (E_F) was also experimentally investigated by means of the low-temperature specific heat and magnetic-susceptibility measurements. The measured electrical resistivity of these approximants is discussed in terms of their local atomic arrangements and the electronic structure near E_F. The factors

introducing the high electrical resistivity both in the approximants and quasicrystals are discussed in detail.

II. EXPERIMENTAL PROCEDURE

Al-Re-Si mother ingots were prepared by melting the constituent elements, Al (purity 99.99%), Re (99.9%), and Si (99.999%), in an arc furnace under a pressurized Ar-gas atmosphere. All mother ingots were molten again in an induction heater and rapidly quenched on a single-role Cu wheel of 18 cm in diameter rotating at 5000 rpm. Ribbon samples thus obtained were annealed at 700 °C for 24 h. The phases in the ribbon samples before and after the heat treatment were determined by a conventional Cu-Kα x-ray-diffraction (XRD) measurement with a commercial diffractometer RIGAKU RINT2000.

The Rietveld analysis was performed on the synchrotron-radiation powder diffraction spectra of $Al_{82.6-x}Re_{17.4}Si_x$ (x $=7$, 9, and 12) accumulated at the beam line BL02B2 in SPring-8, Hyogo, Japan. A wavelength of $\lambda=0.7$ Å, quartz glass capillary tubes of 0.2 mm in diameter, and imaging-plates as the detector were employed with the low-temperature (90 K) nitrogen gas blowing on the sample. We also used the Rietveld analysis on the neutron powder-diffraction spectrum for $Al_{73.4}Re_{17.6}Si_9$ to clearly distinguish the position of Si from that of Al. The neutron-diffraction spectrum was measured at HERMES in KEK, Tsukuba, Japan. The Rietveld program RIETAN2000 developed by Izumi[12] was employed both for the synchrotron-radiation and neutron Rietveld analyses.

The electrical resistivity of the present samples was measured in the temperature ranges from 2 K to 300 K with a conventional four-probe method in the Physical Properties Measurement System, Quantum Design PPMS-9L. The low-temperature specific heat was measured under the magnetic field of 0 and 9 T in the temperature range from 0.5 K to 10 K by the relaxation method with the Oxford Instruments MLHC9H. The magnetization of the samples was also measured under the magnetic field up to 9 T in the temperature range from 2 K to 400 K with a superconducting quantum interference device (SQUID) magnetometer, Quantum Design MPMS-7.

III. RESULTS

A. Composition determination

Figure 1(a) shows a partial composition diagram of the Al-Re-Si alloy system obtained after the heat treatment at 700 °C for 24 h on the rapidly quenched ribbon samples. The typical XRD spectra of the annealed samples are shown in Figs. 2(a) and 2(b). The Al-Re-Si 1/1-1/1-1/1 approximant was obviously stabilized along a composition line indicated as $Al_{82.6-x}Re_{17.4}Si_x$ in the range from $x=7$ to 12, while small but finite amount of secondary phase(s) precipitated in the samples outside of this composition-line. The lattice constant a for the 1/1-1/1-1/1 approximants is shown in Fig. 1(b) as a function of x. Monotonically decreasing a with increasing Si concentration x indicates that Al atoms in the Al-Re-Si 1/1-1/1-1/1 approximant are partially replaced by Si atoms
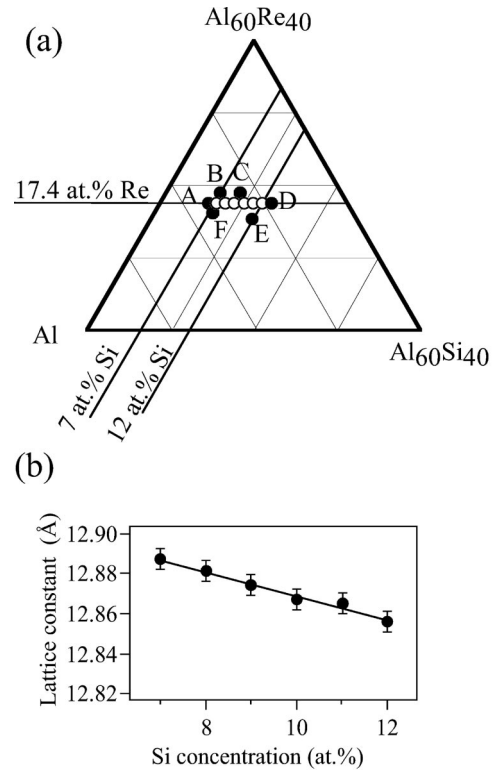

FIG. 1. (a) Partial composition diagram of the Al-Re-Si alloy obtained after a heat treatment of 700 °C for 24 h. Open circles and filled circles indicate the 1/1-1/1-1/1 approximant with and without the precipitation of the secondary phase(s). The compositions in the samples with secondary phase(s) are as follows: A, $Al_{76.6}Re_{17.4}Si_6$; B, $Al_{74.6}Re_{18.4}Si_6$; C, $Al_{72.6}Re_{18.4}Si_6$; D, $Al_{69.6}Re_{17.4}Si_6$; E, $Al_{72.6}Re_{15.4}Si_6$; and F, $Al_{76.6}Re_{16.4}Si_6$. (b) Si concentration dependence of the lattice constant of the $Al_{82.6-x}Re_{17.4}Si_x$ 1/1-1/1-1/1 approximant. The lattice constant a decreases monotonically with increasing x.

without breaking the crystal structure of the 1/1-1/1-1/1 approximant. In sharp contrast with substitutability between Al and Si, Re concentration in the Al-Re-Si 1/1-1/1-1/1 approximant was kept rigidly constant at 17.4 at. % Re. Cooper and Robinson[13] reported that the Al-Mn-Si α-phase known as the 1/1-1/1-1/1 approximant involves totally 138 atom positions in the unit cell. The limited Re concentration only at 17.4 at. % Re reflects the fact that 24 atom positions in the unit cell are exclusively occupied by Re atoms, while Al and Si atoms fill the remaining 114 atom positions. Indeed this idea was clearly confirmed in the result of present Rietveld analysis, that will be discussed in detail later.

The formation area of the stable Al-Re-Si 1/1-1/1-1/1 approximant determined in this study is inconsistent with that reported by Tamura *et al.*,[6] who claimed that the Al-Re-Si 1/1-1/1-1/1 approximant was stabilized over a wide composition range extended towards smaller Re concentration. It should be pressed that we employed the step-scanned data accumulation method with large signal to noise (S/N) ratio to avoid misjudging whether the impurity phases exist in the sample. Invariable concentration of transition metals reported for the other 1/1-1/1-1/1 approximants lends a support to the limited Re concentration in the Al-Re-Si 1/1-1/1-1/1 approximant.[14–16]
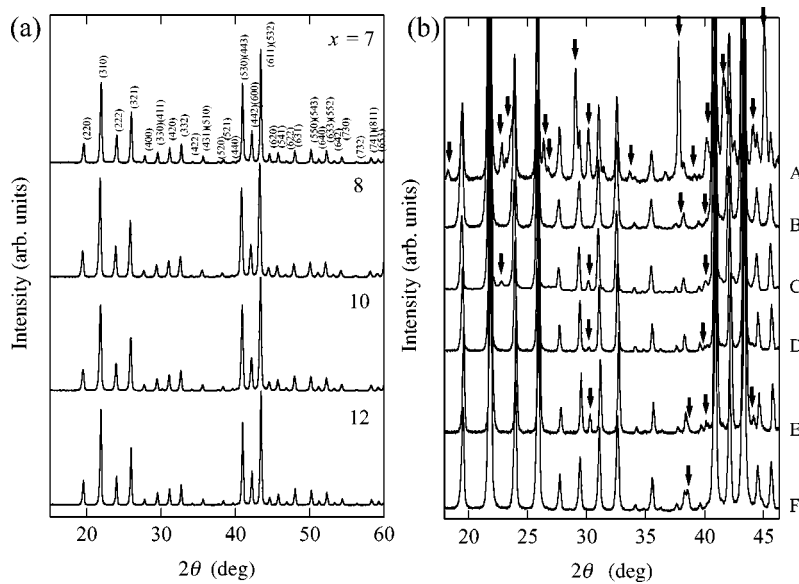
FIG. 2. (a) XRD spectra of the $Al_{82.6-x}Re_{17.4}Si_x$ 1/1-1/1-1/1 approximant ($x = 7$, 8, 10, and 12). These compounds possess no secondary phase. (b) XRD spectra of the samples denoted as $A - E$ in Fig. 1(a). The arrows indicate the diffraction peaks belonging to the secondary phase(s).

B. Structure analysis

Synchrotron-radiation Rietveld analysis was performed on the three samples of different compositions; $Al_{82.6-x}Re_{17.4}Si_x$ ($x = 7$, 9, and 12). If all Mn atoms in the Al-Mn-Si α phase reported previously[13,17,18] are replaced by Re, we obtain almost the same composition as that revealed for the present Al-Re-Si approximant. Therefore the structure of Al-Mn-Si α-phase reported by Cooper and Robinson[13] was used as the initial structure model for the present Rietveld analysis.

Figures 3(a)–3(c) show measured and calculated diffraction spectra obtained after the Rietveld analysis for these three alloys. The resulting structure parameters and reliable factors (R factors[19]) are listed in Table I. By recognizing (1) good agreement between the calculated spectra and the measured ones, (2) good coincidence of the calculated compositions with the nominal ones, and (3) very small R factors, we regarded that the local atomic arrangements in these approximants were successfully determined in the present Rietveld analysis.

As a result of the synchrotron-radiation Rietveld analysis, all Al-Re-Si 1/1-1/1-1/1 approximants were found to have disorder-free Mackay icosahedral (MI) clusters at the body center and vertices in their cubic unit cell. These MI clusters are build up with doubly stacked atomic shells; the first shell is small icosahedron made up with 12 Al atoms, and the second icosahedral shell consists of 12 Re atoms at its vertices and 30 Al atoms at the edge centers. Totally 54 atoms, 12 Re and 42 ($=12+30$) Al, construct the MI cluster without any Si atoms in it. If there were no other atoms in the unit cell, the Al-Re-Si 1/1-1/1-1/1 approximant would have the space group $Im\bar{3}$ as that in the $Al_{68}Cu_7(Fe,Ru)_{17}Si_8$ 1/1-1/1-1/1 approximants.[16,20] However, the $Im\bar{3}$ symmetry of the cubic cell is broken down by the presence of three "glue" sites at spaces between the MI clusters. Although the glue sites violate the symmetry of the bcc lattice, the unit cell still has a bcc-like atomic arrangement. This feature leads to a fact that the diffraction peaks having an even number as the
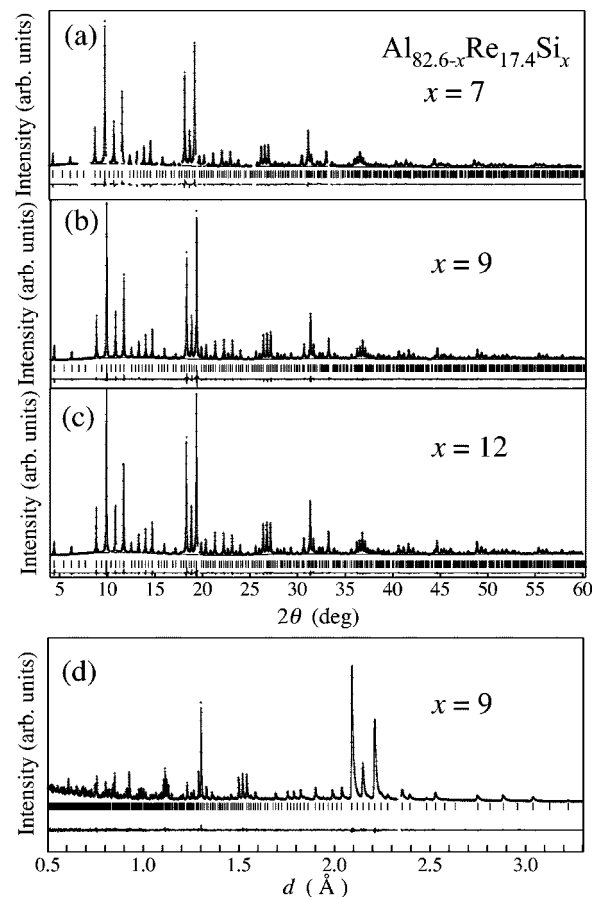

FIG. 3. The fitting result after the Rietveld refinement on the synchrotron-radiation diffraction spectra of (a) $Al_{75.6}Re_{17.4}Si_7$, (b) $Al_{73.6}Re_{17.4}Si_9$, and (c) $Al_{70.6}Re_{17.4}Si_{12}$. (d) Result obtained by the neutron Rietveld analysis for the $Al_{73.6}Re_{17.4}Si_9$. The measured spectra are shown with a marker $+$, and calculated spectra are superimposed on the measured ones. Vertical bars indicate the allowed peak positions. The differences between measured and calculated spectra are shown at the bottom of each panel.

TABLE I. Results of the Rietveld refinement on the $Al_{82.6-x}Re_{17.4}Si_x$ 1/1-1/1-1/1 approximant ($x = 7, 9, 12$).

Cluster	Site	Atoms	Occupancy	x	y	z	$B_{iso.}$ ($Å^2$)
			(a) $Al_{75.6}Re_{17.4}Si_7$, resulting composition $Al_{74.7}Re_{17.6}Si_{7.7}$				
			$a = 12.8605(1)$ Å, $R_{wp} = 2.85\%$, $R_e = 0.76\%$, $R_I = 1.50\%$, $R_F = 0.55\%$				
Inner Ico.	IIa(12j)	Al	1.00	0.163(1)	0.097(1)	0.0000	1.3(1)
	IIb(12k)	Al	1.00	0.350(1)	0.401(1)	0.5000	1.3(1)
Mackay Ico.	MI1a(6e)	Al	1.00	0.363(1)	0.0000	0.0000	0.31(2)
	MI1b(6h)	Al	1.00	0.104(1)	0.5000	0.5000	0.31(2)
	MI2a(24l)	Al	1.00	0.1199(5)	0.181(1)	0.2975(7)	0.31(2)
	MI2b(24l)	Al	1.00	0.3884(6)	0.304(1)	0.1852(9)	0.31(2)
	TMa(12e)	Re	1.00	0.3226(3)	0.1978(2)	0.0000	1.33(1)
	TMb(12h)	Re	1.00	0.1798(3)	0.3023(3)	0.5000	1.33(1)
Glue	G1 (12k)	Al/Si	1.0	0.1294(7)	0.1111(8)	0.5000	0.8(1)
	G2a (6g)	Al	1.0	0.2880(8)	0.0000	0.5000	0.8(1)
	G2b (12j)	Si	0.87(1)	0.3265(7)	0.3988(9)	0.0000	0.8(1)
			(b) $Al_{73.6}Re_{17.4}Si_9$, resulting composition $Al_{73.9}Mn_{17.4}Si_{8.7}$				
			$a = 12.8603(1)$ Å, $R_{wp} = 2.42\%$, $R_e = 0.88\%$, $R_I = 1.81\%$, $R_F = 0.90\%$				
			(Neutron) $R_{wp} = 5.09\%$, $R_e = 4.39\%$, $R_I = 1.64\%$, $R_F = 1.04\%$				
Inner Ico.	IIa(12j)	Al	1.00	0.162(1)	0.095(1)	0.0000	1.15(9)
	IIb(12k)	Al	1.00	0.345(1)	0.399(1)	0.5000	1.15(9)
Mackay Ico.	MI1a(6e)	Al	1.00	0.366(1)	0.0000	0.0000	1.42(6)
	MI1b(6h)	Al	1.00	0.112(1)	0.5000	0.5000	1.42(6)
	MI2a(24l)	Al	1.00	0.1200(7)	0.188(1)	0.3011(9)	1.42(6)
	MI2b(24l)	Al	1.00	0.3903(8)	0.313(1)	0.1956(9)	1.42(6)
	TMa(12e)	Re	1.00	0.3244(2)	0.1986(2)	0.0000	1.36(1)
	TMb(12h)	Re	1.00	0.1807(2)	0.3041(2)	0.5000	1.36(1)
Glue	G1 (12k)	Al	1.00	0.1254(6)	0.1114(7)	0.0000	1.0(1)
	G2a (6g)	Al	1.00	0.3004(9)	0.0000	0.5000	1.0(1)
	G2b (12j)	Si	1.00	0.3260(6)	0.4022(7)	0.0000	1.0(1)
			(c) $Al_{70.6}Re_{17.4}Si_{12}$, resulting composition $Al_{69.7}Re_{17.7}Si_{12.6}$				
			$a = 12.8501(1)$ Å, $R_{wp} = 2.27\%$, $R_e = 1.51\%$, $R_I = 1.34\%$, $R_F = 0.58\%$				
Inner Ico.	IIa(12j)	Al	1.00	0.156(1)	0.092(1)	0.0000	1.09(8)
	IIb(12k)	Al	1.00	0.3373(9)	0.397(1)	0.5000	1.09(8)
Mackay Ico.	MI1a(6e)	Al	1.00	0.368(2)	0.0000	0.0000	1.18(5)
	MI1b(6h)	Al	1.00	0.120(2)	0.5000	0.5000	1.18(5)
	MI2a(24l)	Al	1.00	0.1208(5)	0.1894(7)	0.3009(7)	1.18(5)
	MI2b(24l)	Al	1.00	0.3925(6)	0.3132(8)	0.1921(7)	1.18(5)
	TMa(12e)	Re	1.00	0.3247(2)	0.1970(2)	0.0000	1.24(2)
	TMb(12h)	Re	1.00	0.1806(1)	0.3052(2)	0.5000	1.24(2)
Glue	G1 (12k)	Al	0.82(2)	0.1233(8)	0.1111(7)	0.0000	1.00(9)
	G2a (6g)	Al	1.00	0.2957(9)	0.0000	0.5000	1.00(9)
	G2b (12j)	Al/Si	0.8/0.1(1)	0.3323(7)	0.4029(7)	0.000	1.00(9)

sum of three indices are very intense in sharp contrast with weak peaks with an odd number.

The glue sites are composed of three different atomic sites labeled as G1, G2a, and G2b sites, which have 12, 6, and 12 positions in the unit cell, respectively. No Re atom exists in these three glue sites. Thus the number of atomic positions in the unit cell turns out to be 138 ($= 54 \times 2 + 12 + 12 + 6$), and the Re concentration in this approximant is restricted exactly at $24/138 \cong 17.4$ at. %.

Notably, the sample with $x = 9$ has no disordering even in the glue sites, while weak but finite disordering is introduced in the glue sites with increasing or decreasing Si concentration from $x = 9$. In other words, the disordering becomes more significant if the composition of the 1/1-1/1-1/1 approximant moves away from $x = 9$. We confirmed that the introduced disordering certainly affects the electrical resistivity, and shall return to this point in Discussion.

If the diffraction spectrum is accumulated with a very large S/N ratio, small but finite difference in the photon-interaction-cross-section between Al and Si gives us a reliable information about the positions of Si and Al. As a result of the present synchrotron-radiation Rietveld analysis with
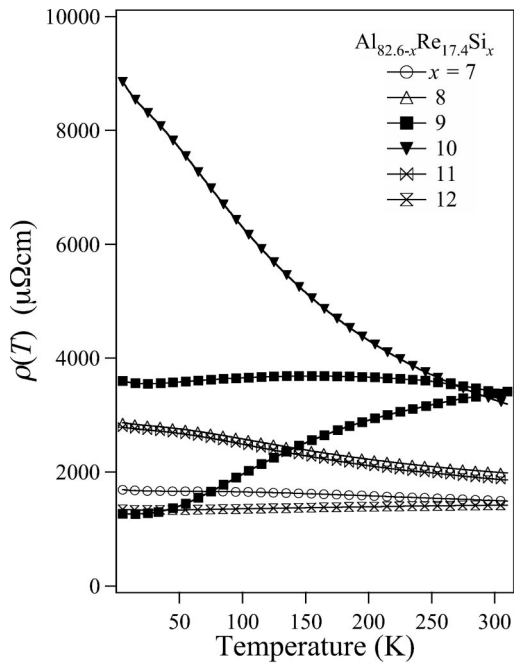
FIG. 4. Temperature dependence of the electrical resistivity for the $Al_{82.6-x}Re_{17.4}Si_x$ ($x=7$, 8, 9, 10, 11, and 12) 1/1-1/1-1/1 approximant. Some ribbons with $x=9$ shows a positive and negative temperature coefficient of resistivity (TCR), while those in other batch possess a negative TCR.

an extremely large S/N ratio, we confidently determined that Si atoms exist only in the glue sites. This result is consistent with our previously reported results on the Al-Cu-Fe-Si, Al-Cu-Ru-Si, and Al-(Mn, Fe)-Si 1/1-1/1-1/1 approximants.[14,16,20]

To obtain a further persuadable evidence for the absence of Si in the MI clusters, the neutron Rietveld analysis was also performed on the disorder-free $Al_{73.6}Re_{17.4}Si_9$ 1/1-1/1-1/1 approximant ($x=9$). The reliable factors obtained by the neutron Rietveld analysis are summarized in Table I together with those obtained by the synchrotron-radiation Rietveld analysis. Although slightly poor data statistics led a slightly larger R_{wp} of 5.09%, the measured neutron-diffraction spectrum was reproduced well and the R_I and R_F were sufficiently reduced below 2% by using the parameters obtained from the synchrotron Rietveld analysis.

C. Electronic properties

Figure 4 shows temperature dependence of the electrical resistivity for the $Al_{82.6-x}Re_{17.4}Si_x$ ($x=7$, 8, 9, 10, 11, and 12) 1/1-1/1-1/1 approximants. A strong composition dependence of the electrical resistivity was observed for these approximants, as had been already reported by Tamura et al.[6] It is very important to note that the strong composition dependence of the electrical resistivity is one of the most pronounced characteristics of the quasicrystals possessing high electrical resistivities, such as Al-Pd-Re quasicrystals.

Here we classified these 1/1-1/1-1/1 approximants into three groups by the behavior of their electrical resistivity: (1) Almost temperature-independent electrical resistivity was observed for $x=7$ and 12; (2) enhancement in the electronic
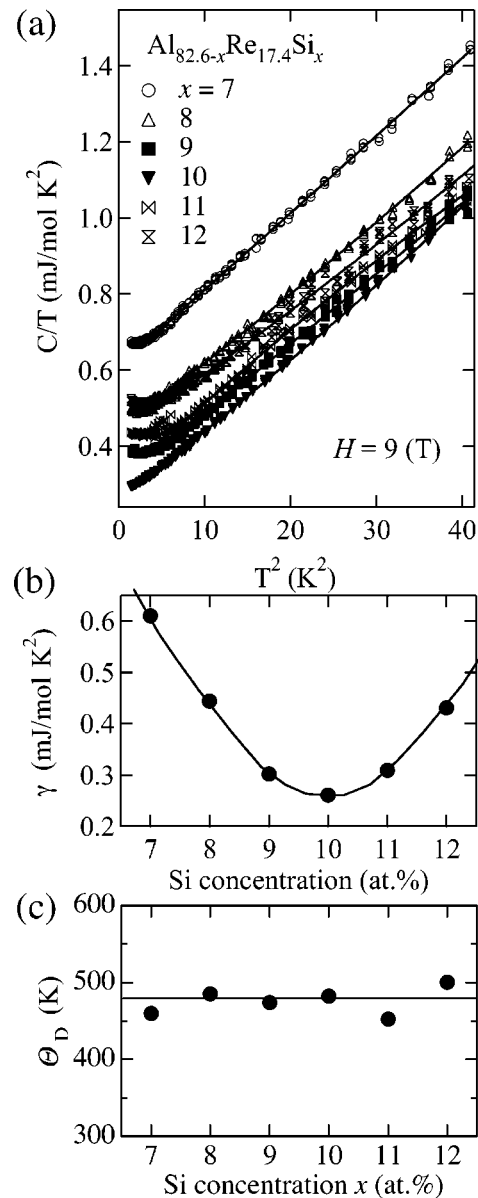

FIG. 5. (a) Low-temperature specific heat of the $Al_{82.6-x}Re_{17.4}Si_x$ ($x=7$, 8, 9, 10, 11, and 12) 1/1-1/1-1/1 approximant measured under the magnetic field of 9 T. (b) Electronic specific-heat coefficient γ deduced as a result of the function fitting on the data measured at 9 T. It shows the minimum value at $x=10$ and increases with increasing or decreasing x. Thus pseudogap formation across E_F is strongly indicated. (c) Debye temperature deduced form α. In sharp contrast to the γ value, almost composition-independent behavior is observed.

resistivity with decreasing temperature was observed at $x=8$, 10, and 11, and it was most pronounced at $x=10$; (3) a positive temperature coefficient of the resistivity was observed only for $x=9$, but the sample with $x=9$ in a different batch showed almost temperature independent electrical resistivity. One may notice that these behaviors in the electrical resistivity in the Al-Re-Si 1/1-1/1 approximants can be roughly sorted with the value of $|9.5-x|$, and is closely related to the density of states at E_F that will be discussed below.

TABLE II. Electron transport properties of the $Al_{82.6-x}Re_{17.4}Si_x$ 1/1-1/1-1/1 approximant.

x	γ (mJ/mol K^2)	α (mJ/mol K^4)	δ (mJ/mol K^6)	Θ_D (K)	χ_{Pauli} (emu/mol)	$\rho_{300\,K}$ ($\mu\Omega$ cm)	RRR
7	0.611(2)	0.0200(2)	$7(5)\times10^{-6}$	459.9(3)	$7.93(4)\times10^{-6}$	1503(70)	1.126
8	0.444(2)	0.0170(2)	$3.7(6)\times10^{-6}$	485.0(5)	$4.14(4)\times10^{-6}$	1998(100)	1.434
9	0.302(3)	0.0183(3)	$4(4)\times10^{-6}$	473.9(6)	$3.73(6)\times10^{-6}$	3403(200)	1.058/0.374
10	0.2612(7)	0.0174(1)	$6.9(3)\times10^{-5}$	482.1(2)	$1.77(7)\times10^{-6}$	3266(190)	2.711
11	0.309(5)	0.0210(5)	$5(1)\times10^{-5}$	452.4(7)	$2.39(2)\times10^{-6}$	1877(95)	1.483
12	0.431(6)	0.0155(7)	$4(1)\times10^{-5}$	500(1)	$5.12(4)\times10^{-6}$	1416(70)	0.9483

Low-temperature specific heat C was measured for the $Al_{82.6-x}Re_{17.4}Si_x$ ($x=7$, 8, 9, 10, 11 and 12) 1/1-1/1-1/1 approximants in the temperature range from 0.5 K to 10 K under the magnetic field up to 9 T. The specific heat C in nonmagnetic systems is in general expressed by the equation $C = \gamma T + \alpha T^3 + \delta T^5$, where γT represents electronic specific heat, and $\alpha T^3 + \delta T^5$ represents the specific heat of the lattice. By dividing both sides of this equation by T, we obtain a formula $C/T = \gamma + \alpha T^2 + \delta T^4$ that is commonly used for analyses on the low-temperature specific heat. The measured specific heat C was divided by T and the resulting C/T values were plotted as a function of T^2 in Fig. 5(a).

Small increase with decreasing temperature, which is hardly explained with the equation described above, was observed below 2 K on the C/T versus T^2 curve of all samples. This increase in C/T at low temperature below 2 K was most likely attributed to the Schottky-type anomaly[21] associated with the magnetic impurities, because the upturn in the C/T versus T^2 curve was reduced and moved towards higher temperature with increasing external magnetic field. To diminish the unfavorable Schottky-type anomaly, we measured specific heat C under the magnetic field of 9 T. The parameters obtained as a result of the function-fitting were listed in Table II. The electronic specific-heat coefficient γ and Debye temperature Θ_D are depicted as a function of Si concentration x in Figs. 5(b) and 5(c), respectively. Obviously, the γ possesses the minimum value at $x=10$, and increases with increasing or decreasing x, while Θ_D was kept almost constant at about 475 ± 25 K.

Since the difference in the atomic numbers between Al and Si is the smallest, the electronic structure and phonon dispersion would be hardly modified by a few at. % substitution of Si for Al even though the electron concentration in the system varies. Almost composition independent Θ_D reflects less significant effects of the substitution of Si for Al. Therefore we consider that the Fermi level moves towards higher or lower binding energies in the almost rigid band with increasing or decreasing x, respectively. The behavior of γ as a function of x indicates the presence of the pseudogap across the Fermi level, and the minimum γ value at $x=10$ means that the Fermi level falls on the bottom of the pseudogap at the vicinity of this particular Si concentration.

Information about the density of states at E_F is also obtained from the Pauli-paramagnetic term in the magnetic susceptibility χ. Figure 6(a) shows the χ value of $Al_{82.6-x}Re_{17.4}Si_x$ ($x=7$, 8, 9, 10, 11 and 12) 1/1-1/1-1/1 approximants as a function of temperature measured at 9 T. In

the temperature range of $100\leq T\leq300$ K, χ showed an almost temperature-independent behavior. However, it is rapidly increased below 30 K in all samples. This corresponds to the Curie-Weiss behavior caused by the free spins in the magnetic impurities, which may lead to the Schottky-type anomaly in the low-temperature specific-heat data.

It is obvious that χ slightly increases with increasing temperature above 300 K. This behavior was sometimes observed for the icosahedral quasicrystals and their approxi-
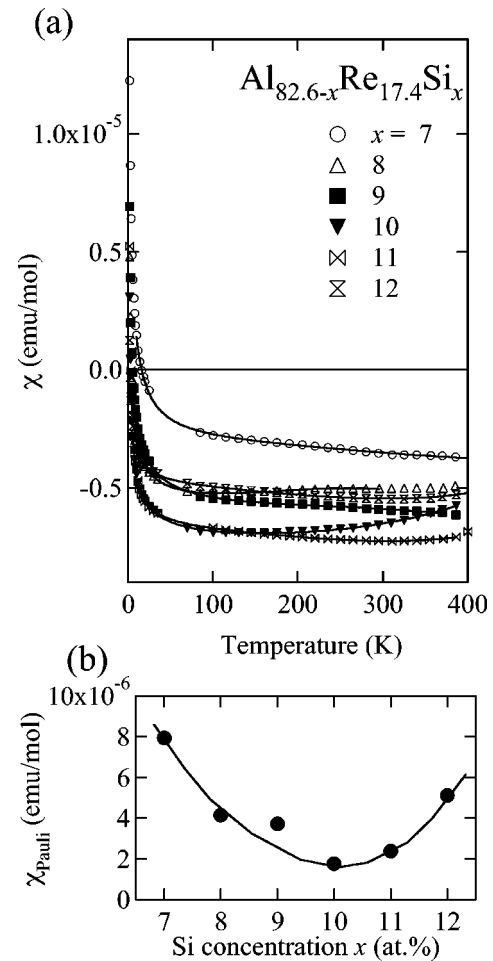

FIG. 6. (a) Temperature dependence of the magnetic susceptibility χ for the $Al_{82.6-x}Re_{17.4}Si_x$ ($x=7$, 8, 9, 10, 11, and 12) measured under the magnetic field of 5 T. (b) Temperature independent χ_{Pauli}. It shows almost the same composition dependence of that in the electronic specific-heat coefficient γ.

mants. Kobayashi *et al.*[22] proposed that this increase in χ at high temperature above 300 K is brought about by the second and third terms in the Sommerfeld expansion. According to their analysis, we employed the equation $\chi = \chi_0 + AT^2 + BT^4 + C/(T - \Theta)$ and deduced the temperature-independent term χ_0. Since χ_0 involves the diamagnetic contributions of ions and Landau levels in addition to the Pauli-paramagnetic term, we subtracted ionic term using values of -2×10^6, -12×10^6, and -1×10^6 emu/mol for Al, Re, and Si, respectively. The deduced $\chi_{\text{Pauli}} = (3/2)(\chi_0 - \chi_{ion})$ is depicted in Fig. 6(b). The term 3/2 was introduced to remove the diamagnetic contribution of the Landau levels, which has magnitude as large as 1/3 of χ_{Pauli}. Resulting χ_{Pauli} definitely possesses the minimum value at $x = 10$ in the same way as the electronic specific-heat coefficient γ possesses minimum value at $x = 10$. Although the fitting function we employed in this analysis has not been commonly accepted yet, we believe that the x dependence of the deduced χ_{Pauli} as well as γ lends a support to the presence of a pseudogap across the Fermi level.

IV. DISCUSSION

To theoretically confirm the pseudogap formation across E_F, we calculated the electron density of states by means of the linear muffin-tin orbital with atomic sphere approximation (LMTO-ASA) method on the refined atomic structure of $Al_{73.4}Re_{17.6}Si_9$ 1/1-1/1-1/1 approximant. Detailed procedures of the LMTO-ASA calculation for this alloy have been already reported elsewhere.[23] In this study, we concentrate on explaining the difference between the LMTO-ASA density of states [abbreviated as $N(E)_{\text{LMTO}}$] calculated for $Al_{73.6}Re_{17.4}Si_9$ and that deduced from the electron specific heat γ [abbreviated as $N(E)_\gamma$] of the $Al_{82.4-x}Re_{17.6}Si_x$ ($x = 7, 8, 9, 10, 11$ and 12) 1/1-1/1-1/1 approximants. The $N(E)_{\text{LMTO}}$ near the Fermi level is shown in Fig. 7 together with the $N(E)_\gamma$. The binding energy for $N(E)_\gamma$ was estimated using the free-electron approximation with 3, -0.9, and 4 valence electrons per Al, Re, and Si, respectively. The value of -0.9 electrons per Re was determined so as $N(E)_\gamma$ to be located near the Fermi level. The calculated density of states is characterized by the pseudogap of 200 meV in width and so-called "spiky" peaks, which are introduced by the small size of the first Brillouin zone associated with the large lattice constant. Although an ambiguity in the binding energy still remains, it is worth mentioning here that the $N(E)_\gamma$ agrees well with the $N(E)_{\text{LMTO}}$ near E_F. Thus we argue here that the presence of the pseudogap across E_F is successfully confirmed by our theoretical calculation.

We are now ready to discuss the strong composition dependence of the electrical resistivity for the Al-Re-Si 1/1-1/1-1/1 approximants in terms of their electronic structure and local atomic arrangements. Mott and Kaveh[24] proposed the following equation, on the basis of an equation reported by Kawabata,[25] to account for the electronic conductivity under the weak localization, which is known as a quantum interference effect associated with multiple elastic scattering:
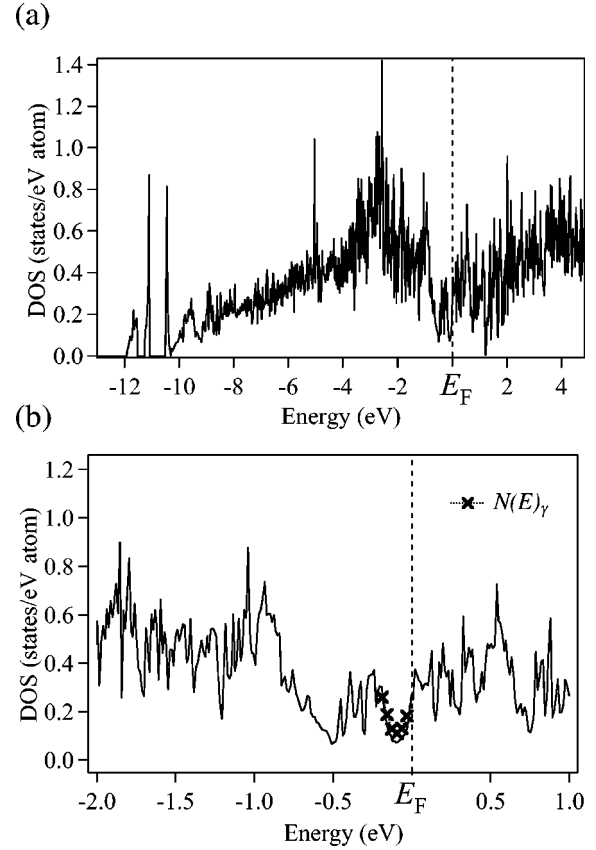
(a)

(b)

FIG. 7. (a) Valence-band density of states calculated for the disorder-free $Al_{73.6}Re_{17.4}Si_6$ 1/1-1/1-1/1 approximant by the LMTO-ASA method. Calculated density of states near E_F $[N(E_F)_{\text{LMTO}}]$ is depicted in (b) and that deduced from the electronic specific-heat coefficient $[N(E_F)_\gamma]$ are superimposed on it.

$$\sigma = \frac{1}{\rho} = \sigma_B \left\{ 1 - \frac{1}{(k_F l)^2} \left(1 - \frac{l}{L} \right) \right\}. \quad (1)$$

Here σ_B, k_F, l, and L represent conductivity deduced from the Boltzmann transport formula, Fermi wave vector, mean free path of elastic scattering, and mean free path of inelastic scattering, respectively.

At high temperatures where L and l become comparable, the second term in the brace obviously disappears and the conductivity is solely determined by the Boltzmann formula, which in an isotropic system is written as

$$\sigma_B = \frac{S_F e^2 l}{12 \pi^3 \hbar} = \frac{e^2}{3} N(E_F) v_F l, \quad (2)$$

where S_F and v_F represent the area of Fermi surface and Fermi velocity, respectively. Only three terms $N(E_F)$, v_F, and l determine the electrical resistivity in this formula. The mean free path l in the Boltzmann equation is expressed as $l = l_{imp} + l_{phonon}$, where l_{imp} and l_{phonon} represent the mean free paths associated with impurity scattering and phonon scattering, respectively. Since the l_{phonon} is much shorter than that of l_{imp} at room temperature, l_{imp} could be safely ignored. Note here that l_{phonon} is scaled by Θ_D, and that almost composition independent Θ_D of the Al-Re-Si 1/1-1/1-1/1 approximant leads to composition independent l_{phonon}

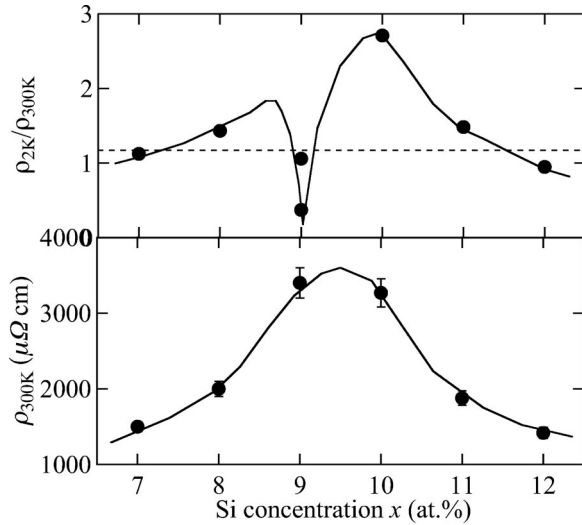FIG. 8. Composition dependence of the residual resistivity ratio defined by $\rho_{2\,K}/\rho_{300\,K}$ and electrical resistivity at room temperature $\rho_{300\,K}$.
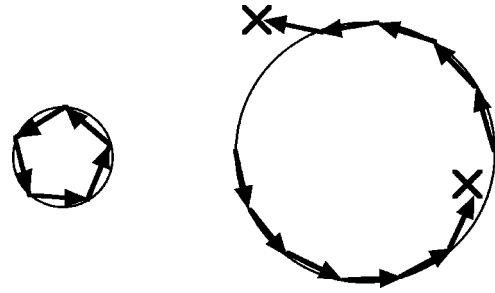

FIG. 9. Schematic drawing of multiple elastic scattering on small and large Fermi surfaces. On the small Fermi surface, multiple elastic scattering easily satisfies a condition for the quantum interference. Quantum interference with the large Fermi surface, on the other hand, is hardly satisfied, because an inelastic scattering would be introduced and destroy the quantum interference before the multiple elastic events round the Fermi surface. When the Fermi surface is large enough, the quantum interference never appears even though the number of the inelastic events is much smaller than that of elastic events.

at room temperature. Therefore composition dependence of the resistivity at room temperature reflects only the composition dependence of the remaining two factors, $N(E_F)$ and v_F. The same result can be concluded under the Ioffe-Riegel limit, where the mean free path of electrons $l = v_F \tau$ is reduced to the averaged interatomic distance $\bar{a}$, and the electrical conductivity turns out to be $\sigma_B^{IR} = (e^2/3)N(E_F)v_F\bar{a}$. The resistivity at room temperature plotted in Fig. 8 actually reflects the composition dependence of the $N(E_F)$; $\rho_{300\,K}$ possesses its maximum value at $x = 9-10$ at.% at which $N(E_F)$ (γ and χ_{Pauli}) shows the minimum value.

We discuss next the electrical resistivity at low temperature, which is closely related to the development of the weak localization. Within the Boltzmann transport equation (2), the temperature dependence of the resistivity is determined by the temperature dependence of the mean free path l; the electrical resistivity increases with increasing temperature because l is reduced by the development of the electron-phonon scattering. On the other hand, when the conduction electrons are strongly affected by the weak-localization effect, the electrical resistivity significantly drops with increasing temperature because enhanced inelastic electron-phonon scattering weakens the weak-localization effect. This is expressed at the second term in the brace of Eq. (1).

Here we introduce a frequently used parameter, the residual resistivity ratio defined as $RRR = \rho_{2K}/\rho_{300\,K}$, to distinguish the electron conduction mechanism in the samples.[5,26] If RRR is kept below 1.1, we consider that the transport mechanism is expressed by the Boltzmann transport equation, while the weak localization takes place at $RRR \geqslant 1.1$.[26] The RRR deduced form the electrical resistivity is plotted in Fig. 8 as a function of Si concentration x. Two peaks and a considerable reduction in RRR are observed at $x = 8$, 10, and 9, respectively. The weak-localization tendency characterized by a large RRR value became obvious for $Al_{82.6-x}Re_{17.4}Si_x$ at $x = 8$ and 10, even though both compounds are expected to have less significant disordering in

the structure because of their compositions lying in the vicinity of the disorder-free $Al_{73.6}Re_{17.4}Si_9$. This is very surprising fact because the weak localization must be brought about by multiple elastic scatterings associated with static disordering in the unit cell.

By carefully comparing the measured properties and structure features, we noticed that the weak localization is more enhanced if the density of states at the Fermi level possesses smaller value even when the disordering in the unit cell is relatively weak. Indeed, the largest RRR value, which means the strongest-localization tendency, is observed for $x = 10$ at which the γ and χ_{Pauli} possess the minimum value.

The small density of states at $N(E_F)$ indicates presence of small Fermi surface(s). In the case with small Fermi surfaces, multiple elastic scattering easily satisfies the condition of the quantum interference. Once the Fermi surfaces get larger, the quantum interference effect should be weakened because an inelastic event prevents the multiple scattering from satisfying the interference condition. This is schematically illustrated in Fig. 9.

The degree of the disordering plays a less important role than the small $N(E_F)$ in enhancing the weak-localization effect. We should stress, however, that the disordering in structure is still one of the necessities for the development of the weak localization for the 1/1-1/1-1/1 approximant, because the disorder-free $Al_{83.6}Re_{17.4}Si_9$ never showed the weak-localization tendency but the Boltzmann-type behavior even though it had a smaller γ value than that of $Al_{84.6}Re_{17.4}Si_8$ possessing a localization tendency. In other words, the Boltzmann-type electron conduction does appear even though the system has fairly small $N(E_F)$, provided that it has a nearly perfect periodic structure.

Obviously, the Boltzmann conductivity σ_B is also strongly reduced by these two crucial factors on the development of the weak localization; the small $N(E_F)$ and imperfection in the periodic structure. Therefore we conclude that the high electrical resistivity in the Al-Re-Si 1/1-1/1-/1/1 approximants is brought about by the small Boltzmann conductivity and the significant weak-localization effect, both of

which are closely related to the small density of states at E_F and imperfection in the periodic structure.

Finally the high electrical resistivities observed for the icosahedral quasicrystals are discussed in comparison with that of the present Al-Re-Si 1/1-1/1-1/1 approximants. We found in this study that the most important factors introducing high electrical resistivity in the Al-Re-Si 1/1-1/1-1/1 approximant are the low density of states at E_F and the imperfection in the periodic structure. In the case of quasicrystals, the condition of the imperfection in the periodic structure is already satisfied because of their possession of quasiperiodicity. Then a small density of states at E_F turns out to be solely responsible for the the high electrical resistivity of the quasicrystals. Indeed the quasicrystals of high electrical resistivity were reported to possess an extremely small γ value; 0.29 mJ/mol K^2 for the Al-Cu-Fe quasicrystal,[27] 0.11–0.2 mJ/mol K^2 for the Al-Cu-Ru quasicrystal,[28] and 0.1 mJ/mol K^2 for the Al-Re-Si quasicrystal.[4] The electrical resistivity at room temperature ($\rho_{300\ K}$) and RRR of these icosahedral quasicrystals are (3000 $\mu\Omega$ cm, 2.0) for Al-Cu-Fe, (5000 $\mu\Omega$ cm, 3.0) for Al-Cu-Ru, and (10000 $\mu\Omega$ cm,10–10 000) for the Al-Pd-Re icosahedral quasicrystal.[5] Obviously those values can be sorted in the order of the γ value; the smaller γ is, the larger ρ_{RT} and RRR are.

Icosahedral quasicrystals of high electrical resistivity, in general, are known to possess a strong composition dependence. For example, a single-grained Al-Pd-Re icosahedral quasicrystal shows an electrical resistivity less than 5000 $\mu\Omega$ cm (Ref. 29) in sharp contrast to the quenched ones possessing more than $10\mu\Omega$ cm at low temperature.[4] This behavior can be also well accounted for by considering our scenario. If the ratio in the constituent elements varies, the electronic structure must be affected. Even if the electronic structure itself is not affected drastically, the Fermi level moves towards higher or lower energies in the pseudogap because of the variation in the electron concentration. This must lead to a variation in the density of sates at the Fermi level, and the degree of the weak localization strongly affected by it. We believe that this is the mechanism for the strong composition dependence in the electrical resistivity of the quasicrystals of high electrical resistivity.

In the case of the Al-Pd-Re icosahedral quasicrystal mentioned above, less resistive single-grained samples[29] have certainly different composition from that of the resistive one.[4] Since Al-Pd-Re quasicrystals are obtained from peritectic reaction, single-grained samples have to be produced from a different composition. Indeed, Fisher $et\ al.$[29] produced single-grained Al-Pd-Re quasicrystals from Al-rich compositions, and the resulting icosahedral quasicrystals also possess a higher Al concentration than that in the samples of a high electrical resistivity. This should be the reason for the relatively low electrical resistivity in the single grained samples. We expect that if the composition is well controlled, the insulating behavior must be observed even in the single-grained Al-Pd-Re icosahedral quasicrystal.

The γ value of the most resistive Al$_{72.6}$Re$_{17.4}$Si$_{10}$ 1/1-1/1-1/1 approximant is comparable with that of the Al-Cu-Fe icosahedral quasicrystal reported by Biggs $et\ al.$[27] It is of great interest to note that these two phases possess similar electrical resistivities in their absolute value and temperature dependence. This fact means that the role of quasiperiodicity in the electrical resistivity is essentially the same with that of disordering in the crystal, and that the degree of the weak localization is solely determined by the magnitude of the small $N(E_F)$ under the presence of the quasiperiodicity in quasicrystal or disordered structure in crystals.

Nearly spherical symmetry of the icosahedral quasicrystal contributes in enhancing electrical resistivity by significantly deepening the pseudogap with the Fermi-surface and Brillouin-zone (FS-BZ) interaction. The effect in deepening pseudogap with the FS-BZ interaction must be stronger in the icosahedral quasicrystal than that in the corresponding approximants, because the icosahedral symmetry in the quasicrystal is more symmetrical than that in approximants. Indeed the electrical resistivity reported for various icosahedral quasicrystals was always higher than that of the corresponding approximants,[7,30] lending a strong support to the scenario of the crucial role of the icosahedral symmetry in enhancing the electrical resistivity.

Structure imperfection of the quasicrystals, in general, is known to reduce their electrical resistivity. This behavior can be also accounted for by considering the FS-BZ interaction. Disordering in the quasicrystals weakens the FS-BZ interaction and makes the pseudogap shallower. Then the density of states at E_F gets larger and the electrical resistivity turns out to be smaller.

V. CONCLUSION

Electrical resistivities in the Al-Re-Si 1/1-1/1-1/1 approximants were investigated and discussed in terms of their electronic structure and the atomic structure. The highest electrical resistivity associated with the strong quantum interference effect is observed at a particular composition of Al$_{72.4}$Re$_{17.6}$Si$_{10.0}$, where the electronic density of states yields the minimum value, while the degree of the disordering in the 1/1-1/1-1/1 approximant was relatively weak. We also observed the disappearance of the weak-localization effect at Al$_{73.6}$Re$_{17.4}$Si$_9$ because of its disorder-free structure. Thus we conclude that the extremely high electrical resistivity characteristic of the icosahedral quasicrystal and corresponding approximants is brought about by the very small density of states at the Fermi level coupled with the imperfections in the periodicity.

[1] A.P. Tsai, A. Inoue, Y. Yokoyama, and T. Masumoto, Mater. Trans., JIM **31**, 98 (1990).

[2] Y. Yokoyama, A.P. Tsai, A. Inoue, T. Masumoto, and H.S. Chen, Mater. Trans., JIM **32**, 421 (1991).

[3] B. Dubost, J.M. Lang, M. Tanaka, P. Sainfort, and M. Audier, Nature (London) **342**, 48 (1986).

[4] F.S. Pierce, Phys. Rev. Lett. **73**, 2220 (1994).

[5] Ö. Rapp, in *Physical Properties of Quasicrystals*, edited by Z. M. Stadnik (Springer, Berlin, 1998), Chap. 5, pp. 127–162.

[6] R. Tamura, T. Asao, and S. Takeuchi, Phys. Rev. Lett. **86**, 3104 (2001).

[7] T. Takeuchi and U. Mizutani, Phys. Rev. B **52**, 9300 (1995).

[8] R. Tamura, Y. Murao, S. Takeuchi, K. Tokiwa, T. Watanabe, T.J. Sato, and A.P. Tsai, Jpn. J. Appl. Phys., Part 2 **40**, L912 (2001).

[9] I.R. Fisher, K.O. Cheon, A.F. Panchula, P.C. Canfield, M. Chernikov, H.R. Ott, and K. Dennis, Phys. Rev. B **59**, 308 (1999).

[10] S. Kashimoto, H. Nakano, Y. Arichika, T. Ishimasa, and S. Matsuo, Mater. Sci. Eng. **294−296**, 588 (2000).

[11] V. Elser and L. Henley, Phys. Rev. Lett. **55**, 2883 (1985).

[12] F. Izumi, Int. Union Crystallogr. **20**, 22 (1998).

[13] M. Cooper and K. Robinson, Acta Crystallogr. **20**, 614 (1996).

[14] T. Takeuchi, T. Onogi, E. Banno, and U. Mizutani, Mater. Trans., JIM **42**, 933 (2001).

[15] T. Takeuchi, H. Yamada, M. Takata, T. Nakata, N. Tanaka, and U. Mizutani, Mater. Sci. Eng. **294−296**, 340 (2000).

[16] T. Takeuchi and U. Mizutani, J. Alloys Compd. **342**, 416 (2002).

[17] K. Sugiyama, N. Kaji, and K. Hiraga, Acta Crystallogr., Sect. C: Cryst. Struct. Commun. **54**, 445 (1998).

[18] K. Kirihara, T. Nakata, M. Takata, Y. Kubota, E. Nishibori, K. Kimura, and M. Sakata, Phys. Rev. Lett. **85**, 3468 (2000).

[19] R. A. Young, *The Rietveld Method*, edited by R. A. Young (Oxford University Press, Oxford, 1993), Chap. 1.

[20] U. Mizutani, T. Takeuchi, E. Banno, V. Fournee, M. Takata, and H. Sato, in *Quasicrystals—Preparation, Properties and Applications*, edited by E. Belin-Ferré, P. A. Thiel, A.-P. Tsai, and K. Urban, MRS Symposia Proceedings No. 643 (Materials Research Society, Pittsburgh, 2001), pp. K13.1.1–K13.1.10.

[21] E. S. R. Gospel, *Specific Heat at Low Temperatures* (Plenum Press, New York, 1966), pp. 102–105.

[22] A. Kobayashi, S. Matsuo, T. Ishimasa, and H. Nakano, J. Phys.: Condens. Matter **9**, 3205 (1997).

[23] T. Onogi, T. Takeuchi, H. Sato, and U. Mizutani, J. Alloys Compd. **342**, 397 (2002).

[24] N.F. Mott and M. Kaveh, Philos. Mag. B **47**, L9 (1983).

[25] A. Kawabata, Solid State Commun. **38**, 823 (1981).

[26] T. Takeuchi, E. Banno, T. Onogi, T. Mizuno, T. Sato, V. Fournee, and U. Mizutani, in *Quasicrystals—Properties and Applications*, edited by E. Belin-Ferré, P. A. Thiel, A.-P. Tsai, and K. Urban, MRS Symposia Proceedings No. 643 (Materials Research Society, Pittsburgh, 2001), pp. K13.4.1–K13.4.6.

[27] B.D. Biggs, Y. Li, and S.J. Poon, Phys. Rev. B **43**, 8747 (1991).

[28] B.D. Biggs, S.J. Poon, and N.R. Munirathnam, Phys. Rev. Lett. **65**, 2700 (1990).

[29] I.R. Fisher, X.P. Xie, I. Tudosa, C.W. Gao, C. Song, P.C. Canfield, A. Kracher, K. Dennis, D. Abanoz, and M.J. Kramer, Philos. Mag. B **82**, 1089 (2002).

[30] R. Tamura, K. Komatsu, T. Asao, and S. Takeuchi, Mat. Sci. Eng **294−296**, 607 (2000).